

**Hydrophobic-Interaction-Induced Stiffening of  $\alpha$ -Synuclein Fibril Networks**Slav A. Semerzhiev,<sup>1</sup> Saskia Lindhoud,<sup>1</sup> Anja Stefanovic,<sup>1</sup> Vinod Subramaniam,<sup>2</sup>  
Paul van der Schoot,<sup>3</sup> and Mireille M. A. E. Claessens<sup>1,\*</sup><sup>1</sup>*Nanobiophysics, MESA+ Institute for Nanotechnology and MIRA Institute for Biomedical Technology and Technical Medicine, University of Twente, P.O. Box 217, 7500 AE Enschede, The Netherlands*<sup>2</sup>*Vrije Universiteit Amsterdam, De Boelelaan 1105, 1081 HV Amsterdam, The Netherlands*<sup>3</sup>*Theory of Polymers and Soft Matter, Eindhoven University of Technology, P.O. Box 513, 5600 MB Eindhoven, The Netherlands*

(Received 15 November 2017; revised manuscript received 14 February 2018; published 17 May 2018)

In water, networks of semiflexible fibrils of the protein  $\alpha$ -synuclein stiffen significantly with increasing temperature. We make plausible that this reversible stiffening is a result of hydrophobic contacts between the fibrils that become more prominent with increasing temperature. The good agreement of our experimentally observed temperature dependence of the storage modulus of the network with a scaling theory linking network elasticity with reversible cross-linking enables us to quantify the endothermic binding enthalpy and estimate the effective size of hydrophobic patches on the fibril surface. Our findings may not only shed light on the role of amyloid deposits in disease conditions, but can also inspire new approaches for the design of thermoresponsive materials.

DOI: [10.1103/PhysRevLett.120.208102](https://doi.org/10.1103/PhysRevLett.120.208102)

Hydrophobic interactions (HIs) play a central role in biology: they often facilitate proteins in attaining their functional form by supporting their native fold or by binding to partners [1,2]. Additionally, HIs help biological macromolecules assemble into complex functional structures. In an intricate interplay with other types of non-covalent interactions, HIs drive the self-assembly of virus coat proteins into virus capsids [3]. This phenomenon has inspired the field of bionanotechnology to create novel self-assembled biosynthetic structures [4,5]. HIs are, however, not only important in a functional context, they have also been implicated in promoting the self-assembly of proteins into oligomeric species and amyloid fibrils, a process accompanying many disease conditions [6].

A distinguishing hallmark of HIs is their nontrivial dependence on temperature. For small hydrophobic solutes as well as large ones characterized by small hydrophobic patches, below, say, 1 nm<sup>2</sup>, HIs become stronger with increasing temperature [7]. This characteristic feature of HIs persists in liquid water and distinguishes HIs from all other types of noncovalent attractive interactions that become effectively weaker at higher temperature. Apart from being a characteristic feature of HIs, the unique temperature response makes this type of noncovalent

interaction a suitable tool to manipulate the properties of materials that have exposed patches of hydrophobic surface. Nevertheless, controlling material properties through hydrophobic forces remains a challenge, arguably resulting from our limited understanding of HIs and the lack of design principles for the synthesis of tunable materials, the responsiveness of which is based on HIs.

Here, we make use of the neuronal protein  $\alpha$ -synuclein ( $\alpha$ S) that under disease conditions self-assembles into amyloid fibrils, and take it as a model system in which material properties can be controlled by harnessing HIs. This protein exhibits a complex phase behavior and, depending on the physicochemical conditions, organizes into hierarchical suprafibrillar aggregates with varying morphologies or into isotropic semiflexible amyloid networks [8,9]. We carefully choose the experimental conditions to steer the self-assembly into the region of the phase diagram where semiflexible networks are formed. Fibril networks are a convenient platform to convincingly address the hydrophobic nature of the attractive interactions that drive the self-organization of  $\alpha$ S fibrils into larger-scale structures. Understanding the nature of the attractive interfibril interactions will help in identifying the role and formation mechanism of pathological fibril structures such as Lewy bodies that accompany the progression of Parkinson's disease. Additionally, the obtained knowledge on how hydrophobic interactions can tune the mechanical properties of a material may inspire design principles for the creation of novel temperature responsive materials. We use temperature as a "tuning knob" to adjust the effective degree of cross-linking in the  $\alpha$ S fibril network, and by

*Published by the American Physical Society under the terms of the Creative Commons Attribution 4.0 International license. Further distribution of this work must maintain attribution to the author(s) and the published article's title, journal citation, and DOI.*

doing so change the viscoelastic response of the material without forcing any permanent structural and associated mechanical alterations in the material. Finally, we quantitatively connect the thermally induced enhancement of HIs to the observed stiffening in the viscoelastic response of the network by incorporating the effect of reversible cross-linking in established scaling theory for semiflexible networks.

The polymerization of  $\alpha S$  into amyloid fibrils is a slow process. Within 7 days after the initiation of polymerization, a solution of monomeric  $\alpha S$  typically evolves into a gel (Fig. S1) [10]. It takes up to 37 days until all the protein has polymerized into fibrils (Fig. S2) [12], stresses in the network are relaxed, and the network has equilibrated [Fig. 1(a)]. Rheologically, the equilibrated networks of semiflexible amyloid fibrils behave as viscoelastic materials. Frequency sweeps of aged networks produce relatively featureless spectra. No crossovers between the frequency-dependent storage modulus  $G'(f)$  and loss modulus  $G''(f)$  are observed in the probed frequency range [Fig. 1(a)]. The

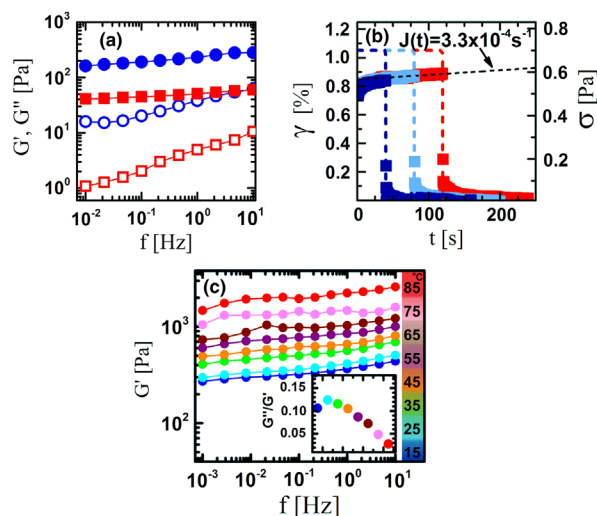


FIG. 1. Rheology on  $\alpha S$  amyloid networks. (a) Frequency sweeps for a 7 days (solid square) and 37 days (solid circle) old sample. The storage modulus and the loss modulus are designated with closed and open symbols, respectively. (b) Creep-recovery tests for an equilibrated  $300 \mu\text{M}$   $\alpha S$  amyloid network. Squares designate the measured strain and the dashed block pulses represent the loading stages characterized by their duration and the amount of stress (0.7 Pa) applied. Squares and dashed lines with different colors are used to discern the measured strain and the duration of the applied stress, respectively, for the 3 subsequent creep-recovery tests with increasing duration of the loading stage. The same sample was used for the three measurements. The estimate for the creep compliance is obtained from the slope of the dashed line. (c) Frequency sweeps for an equilibrated network subjected to an extended temperature treatment. Inset: The damping factor  $G''/G'$  ( $\tan \beta$ ) at 1 Hz as a function of temperature. The decreasing value of the damping factor shows an increase in the elastic portion of the mechanical response of the network.

amyloid network properties are dominated by the storage modulus, as is characteristic for viscoelastic solids. Both  $G'$  and  $G''$  are weakly dependent on the frequency, a feature typical of cross-linked polymeric materials. However, since the  $\alpha S$  amyloid networks are not chemically cross-linked, this observation implies significant attractive interfibril interactions that physically cross-link the fibrils. The presence of associative interfibril interactions is further supported by creep-recovery experiments [Fig. 1(b)]. Applying a constant stress on an  $\alpha S$  fibril network initially induces a time-dependent strain response of the material. Shortly after the stress is applied, the change in the strain reaches a steady state known as creep. The  $\alpha S$  fibril gel exhibits very low creep [Fig. 1(b)], which is again in line with the presence of (localized) attractive interfibril interactions. Once the stress is removed, the network shows very low levels of plastic deformation and recovers almost completely to its original state. The same behavior is observed after extending the period during which the sample is subjected to stress [Fig. 1(b)].

Given the triblock copolymerlike architecture of the  $\alpha S$  monomer, consisting of an amphiphilic domain, a hydrophobic domain, and a net charged domain, it is not surprising that this protein exhibits multiple modes of intermolecular interactions. While the stability of the amyloid fibrils is provided by hydrogen bonding, the driving force for the self-assembly into amyloid fibrils is believed to be hydrophobic interactions. The latter most probably also play a role in interfibril interactions [6]. Considering that the  $\alpha S$  amyloid fold results from the subtle interplay of electrostatic interactions between the charged domains, hydrogen bonding, and HIs, the minimum free-energy conformation of the protein in the fibrils does not preclude some residual exposure of hydrophobic domains that can mediate HIs between fibrils [13]. The formation of  $\alpha S$  fibril clusters after a high-temperature treatment of fibril suspensions indicates that HIs are indeed also involved at the interfibril level [8]. Plausibly, HIs are also responsible for the observed viscoelastic behavior of  $\alpha S$  networks [Fig. 1(a)].

In the right settings, HIs can be made stronger by elevating the temperature of the system [7]. If HIs are indeed responsible for interfibril interactions in  $\alpha S$  amyloid networks, temperature should have a pronounced effect on the viscoelastic response of the network to applied deformation. Indeed, an  $\alpha S$  network significantly stiffens in the temperature range from 15 to 85 °C, which expresses itself in an order of magnitude increase of the storage modulus  $G'$  [Fig. 1(c)]. This temperature-induced network stiffening is reversible. The value of  $G'$  tightly follows the changes in the temperature even if the network is repeatedly subjected to temperature cycles with different amplitudes (Fig. S3) [14]. This behavior is typically not observed in networks of semiflexible polymers, yet does superficially resemble the elastic behavior of rubbers. In the latter, the free-energy

cost of stretching out the stored contour length of the cross-linked polymers becomes much larger at elevated temperatures, an effect associated with them being flexible rather than semiflexible. However,  $\alpha S$  fibrils formed at the conditions used to prepare the amyloid gels appear to be very stiff, as is evidenced by total internal reflection microscopy (TIRF) images [Fig. S4(a)] [15]. An end-to-end distance versus contour length analysis of the fibrils yields an estimate for the persistence length of  $l_p \approx 85 \mu\text{m}$ , which is very much larger than the mesh size expected for a  $300 \mu\text{M}$   $\alpha S$  fibril network [Figs. S4(b) and S4(c)] [15]. It is therefore unlikely that the increased free-energy cost of reducing the conformational freedom of an individual fibril contributes significantly to the observed increase in  $G'$  with increasing temperature.

A huge experimental and theoretical research effort has been invested in the past few decades to better understand the viscoelastic properties of networks composed of semiflexible polymers [17]. These efforts have resulted in theoretical frameworks that describe scaling relations between quantities characterizing the properties of these networks, and which have been successfully applied to a wide range of biological and synthetic materials, all falling in the general class of semiflexible polymer networks [18–20]. In view of the featureless frequency sweeps and the creep-recovery experiments, the  $\alpha S$  fibril network seems to behave as a cross-linked network [Fig. 1(a)]. With this in mind, we have adopted the scaling theory for cross-linked semiflexible networks in order to interpret the temperature behavior of the  $\alpha S$  amyloid network. Because of the relatively large persistence length of  $\alpha S$  fibrils compared to the mesh size, we invoke a scaling theory based on the so-called floppy modes model, assuming a constant strain [21].

According to this model, we have

$$G'_0 \sim \frac{\kappa}{\xi^2 l_c^4}, \quad (1)$$

where  $G'_0$  is the plateau modulus of the network,  $\kappa$  is the bending stiffness of the semiflexible chains,  $\xi$  the average mesh size, and  $l_c$  the average distance between cross-links [22] [see also Fig. 2(b)]. Note that the persistence length and bending stiffness are related according to  $l_p = \kappa/k_B T$ . The strong dependence of the plateau modulus on the number of cross-links (through  $l_c$ ) is apparent. However, before focusing on this particular quantity, the possible contribution of the other two relevant parameters to the observed thermal stiffening in  $\alpha S$  networks, namely  $\xi$  and  $\kappa$ , needs to be considered. Large temperature-induced stiffening of semiflexible polymers has been observed in some synthetic systems. Driven by the enhanced hydrophobic interactions at higher temperatures, synthetic polymers may bundle into filaments with more than an order of magnitude larger rigidity [20]. The enhancement of  $\kappa$  can in

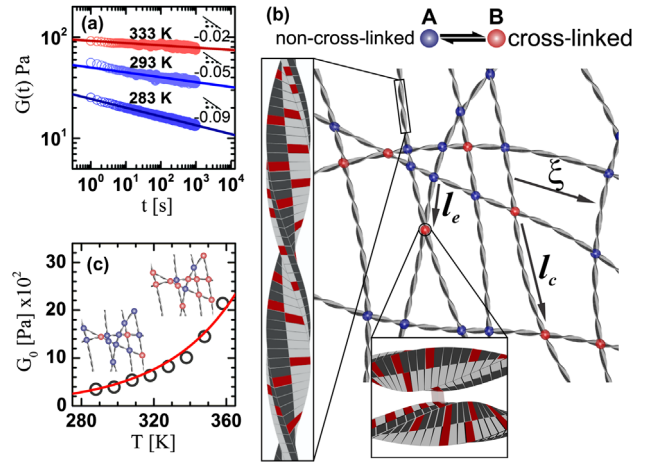


FIG. 2. Hydrophobically cross-linked  $\alpha S$  amyloid networks. (a) Stress-relaxation tests of a  $300 \mu\text{M}$   $\alpha S$  network ( $2 \text{ mM Na}^+$ ) at different temperatures. The stress-relaxation curves are vertically shifted for a better visualization. (b) Artist impression of a “hydrophobically cross-linked”  $\alpha S$  amyloid network. The tentative hydrophobic patches on the surface of the fibrils are presented in red. (c) Scaling of the storage modulus with temperature. The circles represent the experimental data, the red curve is the fit generated using the scaling relation derived in the Supplemental Material [Eq. (2)] [34]. Cartoon insets: At higher temperature the number of effective cross-links is significantly higher as compared to lower temperatures.

that case be large enough to overcome the effect of the increased mesh size, which is expected to soften the network [Eq. (1)] and to produce an overall increase in the plateau modulus [23]. Even though hydrophobic interactions also seem to play an important role at the intra- and interfibril level in  $\alpha S$  networks, bundling is an unlikely mechanism to account for the experimental observations at higher temperatures. Small-angle x-ray scattering (SAXS) measurements do not provide any evidence for significant structural changes in the  $\alpha S$  network at these higher temperatures. The fibril cross sections remain close to constant throughout the temperature ramps [Figs. S4(d) and S4(e)] [24]. Moreover, the SAXS curves remain identical at the different temperatures, indicating that there are no sizable changes in the overall structure of the network and consequently in the mesh size  $\xi$ .

If bundling does not take place, then the strong temperature dependence of  $G'_0$  might result from a drastic change in the bending rigidity of the individual fibrils themselves with temperature. Since  $G'_0 \sim \kappa$  [Eq. (1)], the observed change in  $G'_0$  between  $5^\circ\text{C}$  and  $80^\circ\text{C}$  would imply a 13-fold increase over that temperature range. This estimate is based solely on changes in  $\kappa$  without taking into account the changes in the so-called entanglement length  $l_e$ . If the sensitivity of  $l_e$  on the temperature is also taken into account, using the known scaling relations and assuming cross-links can only appear at entanglement points  $l_c \sim l_e \sim l_p^{1/5} \sim (\kappa/k_B T)^{1/5}$ , then the increase of  $\kappa$  with

temperature would need to be even larger [Eq. (1)] [26]. The temperature dependence of  $\kappa$  is, however, generally very moderate for semiflexible biopolymers. Additionally, the sign of the change strongly depends on the biopolymer species. While, depending on guanine-cytosine content and salt concentration, double-stranded DNA seems to exhibit a 15%–20% reduction in  $\kappa$  with increasing the temperature from 30 °C to 45 °C, single-stranded DNA shows a 15% increase of  $\kappa$  over a comparable temperature range [27–29]. A drastic change in the mechanical properties of individual  $\alpha S$  fibrils also seems highly unlikely. As mentioned earlier, the protein monomers in the cross  $\beta$ -sheets fibril backbone are held together by numerous intermolecular hydrogen bonds, which are the main determinant for the fibril stiffness [30].

Driven by inter- and intramolecular HIs,  $\alpha S$  monomers aggregate and attain a fold with optimized internalization of apolar residues in the fibril’s core. Keeping this in mind, higher temperatures stimulate two counteracting effects: on one hand, the breaking of hydrogen bonds should reduce the rigidity of the fibrils, and, on the other, the enhancement of the hydrophobic interaction could increase the stiffness. However, it is unlikely that the strength of intermonomer HIs increases sufficiently to compensate for the loss of hydrogen bonds, and produce the dramatic net increase in  $\kappa$  that would account for the unusual increase in the  $G'_0$  of the network. Indeed, other molecular assemblies that are held together by hydrophobic interactions also do not show signs of unusual stiffening, induced by an increase in temperature in the range comparable to the one used in this study. Lipid bilayers, for example, become easier to deform with increasing temperature [31,32]. The filamentous fd virus exhibits a nonmonotonic change in the persistence length  $l_p = \kappa/k_b T$  with temperature: at higher temperature,  $l_p$  decreases, while an increase is found at the lower temperature range [33]. This variation in  $l_p$  is however small, amounting to no more than 30%.

With changes in  $\kappa$  being an unlikely cause for the large temperature-induced increment of  $G'_0$ , the only parameter left that could potentially account for this phenomenon is the mean distance between cross-links  $l_c$ . Heating up the system seems to strengthen the hydrophobic contacts between the fibrils, which ultimately results in a more densely cross-linked network. Results from stress-relaxation measurements on an  $\alpha S$  network at different temperatures are in line with this hypothesis. Instead of speeding up the relaxation processes, heating up the sample actually slows down the relaxation dynamics [Fig. 2(a)], probably due to the enhanced interfibrillar contacts [Fig. 2(b)].

To test the hypothesis that heating the amyloid network strengthens hydrophobic contacts between fibrils, we establish a quantitative relation between temperature and the storage modulus. For this purpose, we introduce a two state model for the entanglements in the network  $A \rightarrow B$ ,

where  $A$  and  $B$  represent the “free” and “cross-linked” entanglements, respectively [Fig. 2(b)]. Assuming that hydrophobic interactions drive the cross-linking of entanglements, the impact of temperature on the effective number of cross-links in the system is evaluated at the level of a Boltzmann equilibrium and incorporated in the scaling relations for cross-linked semiflexible networks [34]. This results in the following relation:

$$G'_0(T) = G'_0(T_0)e^{(H_0/k_b T_0^2)(T-T_0)} \left(\frac{T_0}{T}\right)^{(2/5)}, \quad (2)$$

where  $G'_0(T)$  is the temperature-dependent plateau modulus and  $G'_0(T_0)$  the plateau modulus at the reference temperature  $T_0$ . The value of  $H_0$  strongly depends on the architecture of  $\alpha S$  fibrils. Since there is no established model for this architecture,  $H_0$  is left as a free parameter. The reference temperature  $T_0 = 288$  K, which is the lowest temperature at which the storage modulus was measured, is used to fit Eq. (2) to the experimental data. Equation (2) seems to describe the experimental observations very well [Fig. 2(c)]. The fit yields an endothermic value for  $H_0 = 7.5k_b T$ . From the obtained value for  $H_0$  we can estimate the apparent size of the hydrophobic patches using the expression for the enthalpy of hydrophobic contacts at the reference state:  $H_0 = 2h_{\text{HI}}a$ , where  $h_{\text{HI}}$  is the energy cost per unit area of exposed hydrophobic surface and  $a$  is the area [39]. Taking into account that typically  $h_{\text{HI}} \sim 7k_b T \text{ nm}^{-2}$ , the estimate for the size of the hydrophobic patches on the fibril surface is  $\sim 0.75 \text{ nm}^2$ , which is comparable to what has been found previously for virus coat proteins [3,39,40].

In summary, equilibrated  $\alpha S$  amyloid networks exhibit remarkable thermoresponsive properties. The fibrillar gel significantly stiffens at higher temperatures and completely recovers its original state once the temperature is lowered again. We show that this stiffening does not result from bundling of fibrils and propose that the thermostiffening of the  $\alpha S$  network is the consequence of enhanced interfibrillar hydrophobic contacts stimulated by the higher temperature. This is consistent with previously established qualitative findings, suggesting that the hydrophobic effect plays an essential role in the interaction between  $\alpha S$  fibrils [8,9,41]. The presence of hydrophobic interactions between fibrils suggest that multiple hydrophobic domains in the fibril core remain solvent exposed. At higher temperatures these hydrophobic areas become “activated,” which effectively increases the number of contact points between fibrils. An alternative explanation in which the exposure of the hydrophobic domains itself is a temperature-induced phenomenon could also be considered [42].

Elucidating the cohesive forces between amyloid fibrils is crucial for obtaining a better understanding of the associated pathology and the physiological role of such structures. A correlation between the exposure of hydrophobic surface

in amyloid aggregates and their toxicity has been suggested by numerous studies [43–45]. Considering the nanoscale organization of the  $\alpha$ S fibrils, it is unlikely that all hydrophobic patches on the fibril surface are protected from contact with the aqueous environment by interfibril interactions. The exposure of these hydrophobic fibril patches to the cytosol may induce interactions with other proteins. The accumulation of additional proteins in amyloid deposits may therefore not be a result of preserved functional interactions but rather be an effect of HIs. The accumulation of amyloid fibrils might increase the total hydrophobic surface present in the cell and thereby interfere with its normal functioning.

Understanding the interfibril interactions is also imperative for the successful utilization and manipulation of amyloid materials. Our data indicate that there are opportunities to harness these interactions and tune the mechanical properties of amyloid materials. Moreover, these findings indicate that it should be possible to design amyloid fibrils or other supramolecular assemblies with engineered hydrophobic patches and synthesize materials with imprinted temperature responsiveness. An important question remains, however. Are these interactions generic for amyloids or just specific for  $\alpha$ S? Exposure of amyloid networks composed of the disease-unrelated protein  $\beta$ -lactoglobulin does not seem to provoke the same response, indicating that the degree of thermostiffening observed for  $\alpha$ S gels cannot be expected to hold for all amyloid materials [46].

This work was supported by the Nederlandse Organisatie voor Wetenschappelijk Onderzoek (NWO) through NWO-CW Veni grant (722.013.013) to S. L., NWO-CW TOP program (700.58.302) to V. S., NWO-CW VIDI grant (700.59.423) to M. M. A. E. C., and through and Nanonex NL theme 8A. The authors thank Kirsten van Leijenhorst-Groener and Nathalie Schilderink for the expression and purification of  $\alpha$ -synuclein. SAXS experiments were performed at ESRF, BM26 (DUBBLE) experiment no. 26-02-664. We thank Dr. G. Portale (Beamline Scientist) for his help performing SAXS experiments.

\*Corresponding author.

m.m.a.e.claessens@utwente.nl

- [1] H. J. Dyson, P. E. Wright, and H. A. Scheraga, *Proc. Natl. Acad. Sci. U.S.A.* **103**, 13057 (2006).
- [2] J. M. Sturtevant, *Proc. Natl. Acad. Sci. U.S.A.* **74**, 2236 (1977).
- [3] W. K. Kegel and P. van der Schoot, *Biophys. J.* **86**, 3905 (2004).
- [4] M. Comellas-Aragones, H. Engelkamp, V. I. Claessen, N. A. J. M. Sommerdijk, A. E. Rowan, P. C. M. Christianen, J. C. Maan, B. J. M. Verduin, J. J. L. M. Cornelissen, and R. J. M. Nolte, *Nat. Nanotechnol.* **2**, 635 (2007).
- [5] A. Hernandez-Garcia, D. J. Kraft, A. F. J. Janssen, P. H. H. Bomans, N. A. J. M. Sommerdijk, D. M. E. Thies-Weesie, M. E. Favretto, R. Brock, F. A. de Wolf, M. W. T. Werten, P. van der Schoot, M. C. Stuart, and R. de Vries, *Nat. Nanotechnol.* **9**, 698 (2014).
- [6] A. K. Buell, A. Dhulesia, D. A. White, T. P. J. Knowles, C. M. Dobson, and M. E. Welland, *Angew. Chem., Int. Ed. Engl.* **51**, 5247 (2012).
- [7] D. Chandler, *Nature (London)* **437**, 640 (2005).
- [8] S. A. Semerdzhiev, D. R. Dekker, V. Subramaniam, and M. M. Claessens, *ACS Nano* **8**, 5543 (2014).
- [9] S. A. Semerdzhiev, V. V. Shvadchak, V. Subramaniam, and M. M. A. E. Claessens, *Sci. Rep.* **7**, 7699 (2017).
- [10] See Supplemental Material at <http://link.aps.org/supplemental/10.1103/PhysRevLett.120.208102> for details about the protein expression and purification, which includes Ref. [11].
- [11] B. D. v. Rooijen, Ph. D. thesis, University of Twente, 2009.
- [12] See Supplemental Material at <http://link.aps.org/supplemental/10.1103/PhysRevLett.120.208102> for the details about Fig. S2 and the temporal evolution of the polymerization of  $\alpha$ S monomers into fibrils.
- [13] M. S. Celej, E. A. Jares-Erijman, and T. M. Jovin, *Biophys. J.* **94**, 4867 (2008).
- [14] See Supplemental Material at <http://link.aps.org/supplemental/10.1103/PhysRevLett.120.208102> for the details about Fig. S3 and the reversible temperature stiffening of  $\alpha$ S amyloid networks.
- [15] See Supplemental Material at <http://link.aps.org/supplemental/10.1103/PhysRevLett.120.208102> for details about the persistence length analysis of  $\alpha$ S fibrils, which includes Ref. [16].
- [16] G. Lamour, H. B. Li, and J. Gsponer, *Biophys. J.* **104**, 393a (2013).
- [17] C. P. Broedersz and F. C. MacKintosh, *Rev. Mod. Phys.* **86**, 995 (2014).
- [18] M. L. Gardel, J. H. Shin, F. C. MacKintosh, L. Mahadevan, P. Matsudaira, and D. A. Weitz, *Science* **304**, 1301 (2004).
- [19] E. M. Huisman, Q. Wen, Y. H. Wang, K. Cruz, G. Kitenbergs, K. Erglis, A. Zeltins, A. Cebers, and P. A. Janmey, *Soft Matter* **7**, 7257 (2011).
- [20] P. H. J. Kouwer, M. Koepf, V. A. A. Le Sage, M. Jaspers, A. M. van Buul, Z. H. Eksteen-Akeroyd, T. Woltinge, E. Schwartz, H. J. Kitto, R. Hoogenboom, S. J. Picken, R. J. M. Nolte, E. Mendes, and A. E. Rowan, *Nature (London)* **493**, 651 (2013).
- [21] C. Heussinger and E. Frey, *Phys. Rev. Lett.* **97**, 105501 (2006).
- [22] O. Lieleg and A. R. Bausch, *Phys. Rev. Lett.* **99**, 158105 (2007).
- [23] R. Tharman, M. M. A. E. Claessens, and A. R. Bausch, *Biophys. J.* **90**, 2622 (2006).
- [24] See Supplemental Material at <http://link.aps.org/supplemental/10.1103/PhysRevLett.120.208102> for more information about the SAXS data analysis, which includes Ref. [25].
- [25] M. V. Petoukhov, D. Franke, A. V. Shkumatov, G. Tria, A. G. Kikhney, M. Gajda, C. Gorba, H. D. T. Mertens, P. V. Konarev, and D. I. Svergun, *J. Appl. Crystallogr.* **45**, 342 (2012).
- [26] H. Isambert and A. C. Maggs, *Macromolecules* **29**, 1036 (1996).
- [27] S. de Lorenzo, M. Ribezzi-Crivellari, J. R. Arias-Gonzalez, S. B. Smith, and F. Ritort, *Biophys. J.* **108**, 2854 (2015).

- [28] S. Geggier, A. Kotlyar, and A. Vologodskii, *Nucleic Acids Res.* **39**, 1419 (2011).
- [29] R. P. C. Driessen, G. Sitters, N. Laurens, G. F. Moolenaar, G. J. L. Wuite, N. Goosen, and R. T. Dame, *Biochemistry* **53**, 6430 (2014).
- [30] A. W. P. Fitzpatrick, G. M. Vanacore, and A. H. Zewail, *Proc. Natl. Acad. Sci. U.S.A.* **112**, 3380 (2015).
- [31] G. Niggemann, M. Kummrow, and W. Helfrich, *J. Phys. II (France)* **5**, 413 (1995).
- [32] J. Pan, S. Tristram-Nagle, N. Kucerka, and J. F. Nagle, *Biophys. J.* **94**, 117 (2008).
- [33] J. X. Tang, S. Wong, P. T. Tran, and P. A. Janmey, *Ber. Bunsen-Ges. Phys. Chem.* **100**, 796 (1996).
- [34] See Supplemental Material at <http://link.aps.org/supplemental/10.1103/PhysRevLett.120.208102> for the derivation of Eq. (2), which contains Refs. [3,35–38].
- [35] P. van der Schoot, in *Supramolecular Polymers*, 2nd ed., edited by A. Ciferri (Taylor & Francis, Boca Raton, FL, 2005), pp. xiii, 761.
- [36] A. T. Dapoian, A. C. Oliveira, and J. L. Silva, *Biochemistry* **34**, 2672 (1995).
- [37] P. G. Degennes, P. Pincus, R. M. Velasco, and F. Brochard, *J. Phys. (Paris)* **37**, 1461 (1976).
- [38] T. Ikenoue, Y. H. Lee, J. Kardos, M. Saiki, H. Yagi, Y. Kawata, and Y. Goto, *Angew. Chem., Int. Ed. Engl.* **53**, 7799 (2014).
- [39] R. Phillips, J. Kondev, and J. Theriot, *Physical Biology of the Cell* (Garland Science, New York, 2009), pp. xxiv, 807.
- [40] D. J. Kraft, W. K. Kegel, and P. van der Schoot, *Biophys. J.* **102**, 2845 (2012).
- [41] A. Iyer, S. Roeters, V. Kogan, S. Woutersen, M. M. A. E. Claessens, and V. Subramaniam, *J. Am. Chem. Soc.* **139**, 15392 (2017).
- [42] See the Discussion section in the Supplemental Material at <http://link.aps.org/supplemental/10.1103/PhysRevLett.120.208102> for a more elaborate discussion on an alternative explanation of the observed temperature response of  $\alpha$ S amyloid networks which contains Ref. [38]
- [43] F. Bemporad and F. Chiti, *Chem. Biol.* **19**, 315 (2012).
- [44] B. Mannini, E. Mulvihill, C. Sgromo, R. Cascella, R. Khodarahmi, M. Ramazzotti, C. M. Dobson, C. Cecchi, and F. Chiti, *ACS Chem. Biol.* **9**, 2309 (2014).
- [45] H. Olzscha, S. M. Schermann, A. C. Woerner, S. Pinkert, M. H. Hecht, G. G. Tartaglia, M. Vendruscolo, M. Hayer-Hartl, F. U. Hartl, and R. M. Vabulas, *Cell* **144**, 67 (2011).
- [46] W. S. Gosal, A. H. Clark, and S. B. Ross-Murphy, *Biomacromolecules* **5**, 2408 (2004).